SLAC-PUB-2121
May 1978
(T/E)

APPLICATIONS OF QCD*

John Ellis
CERN - Geneva, Switzerland
and
Stanford Linear Accelerator Center
Stanford University, Stanford, California 94305

Talk presented at the meeting on "Current Trends in the Theory of Fields" held in honor of Prof. P.A.M. Dirac on the occasion of his 75th birthday and the 50th anniversary of the Dirac equation, at the Florida State University, Tallahassee, Florida 32306, April 6th and 7th, 1978.

*Work supported by the Department of Energy

1. INTRODUCTION

A substantial fraction of the theoretical physics community tends to be rather smug these days. It feels that not only are the weak and electromagnetic interactions known to be combined in a non-abelian gauge theory, but that the theory of the strong interactions is known to be Quantum Chromodynamics (QCD).[1] It is true that there are one or two minor technical problems to be clarified, such as the mechanism by which quarks are confined (if indeed they are), but the riddles of the nuclear interactions are supposed to be solved in principle. All very fine, but the rest of the community is entitled to ask for the positive evidence that QCD is correct. At present much of the evidence is either by default (no other plausible field theory seems capable of asymptotic freedom[2] or confinement) or purely aesthetic (QCD is beautiful, it is a gauge theory as are our theories of the other fundamental interactions) or rather qualitative (charmonium,[3] the approximate validity of the parton model,[4] the Zweig rule,[5] and so on). The community is surely entitled to see some direct experimental confirmation of specific theoretical numbers reliably predicted by QCD.

The purpose of this talk is to review the status of reliable QCD predictions which either have, or soon can be verified by experiment. It is divided into three parts:

1. A discussion of the classic application of QCD perturbation theory and asymptotic freedom to predict scaling violations in deep inelastic leptoproduction experiments.[6] Emphasis will be laid on recent results from the BEBC neutrino collaboration[7] which provide the first direct experimental confirmation of the numerical values of the anomalous dimensions predicted[6] by QCD. These data may constitute the best phenomenological evidence to date in favor of QCD.

2. A review of recent advances in developing and justifying QCD perturbation theory predictions for a number of physical applications not underwritten by the operator product expansion and renormalization group arguments generally used to motivate the application of asymptotic freedom to deep inelastic processes. These include predictions for two- and multi-jet production cross-sections in e^+e^-, lepton-hadron and hadron-hadron collisions[8,9]; a modified Drell-Yan formula for lepton-pair production in hadron-hadron collisions[10]; and scaling violations in hadronic final states[11] analogous to those seen in deep inelastic structure functions. Very few of these predictions have yet been confronted with experiment, but they promise to provide copious, precise and reliable ways to verify or disprove QCD.

3. A final mention will be made of attempts to address the question whether these predictions of QCD perturbation theory should be regarded as reliable, given the fact that non-perturbative effects[12] are presumably crucial in QCD (to confine quarks,[13] for example). Analyses[14] of the simplest non-perturbative corrections to the most basic deep inelastic process $\sigma(e^+e^- \to \gamma^* \to \text{hadrons})$ indicate that they are negligible at large momentum transfers. This suggests that QCD perturbation theory predictions may indeed by reliable for the deep inelastic, large momentum transfer processes where the previously proposed experimental tests are to be made.[15]

2. DEEP INELASTIC SCATTERING

The classic tests of QCD are afforded by deep inelastic leptoproduction. Every field theory predicts that the structure functions should violate scaling as $Q^2 \to \infty$, but QCD makes very specific predictions, owing to the fact that its coupling constant is asymptotically free at large momenta[16]:

$$\alpha_s(Q^2) \equiv \frac{g^2(Q^2)}{4\pi} \overset{Q^2\to\infty}{\simeq} \frac{12\pi}{(33-2N_f)\ln(Q^2/\Lambda^2)} \tag{1}$$

These predictions are expressible most precisely in terms of the Q^2 dependence expected for the moments[17]

$$M_i(N,Q^2) \equiv \int_0^1 dx\, x^{N-2} F_i(x,Q^2) \tag{2}$$

of the deep inelastic structure functions F_i (F_2 and xF_3 will be discussed here). QCD predicts[6] that the moments $M_i(N,Q^2)$ should behave as negative powers of $\log(Q^2/\Lambda^2)$ as $Q^2 \to \infty$, whereas any other field theory would predict power-law violations of scaling.[18] The predictions are simplest for flavor non-singlet structure functions, such as $F_2^{ep}-F_2^{en}$, or the vector-axial vector interference structure function xF_3 measured in charged current νN and $\bar{\nu}N$ scattering. For these cases

$$M_i(N,Q^2) \underset{Q^2\to\infty}{\simeq} C_i^N(\ln Q^2/\Lambda^2)^{-d_N}\left[1+O\left(\frac{1}{\log Q^2/\Lambda^2}, \frac{\log\log Q^2/\Lambda^2}{\log Q^2/\Lambda^2}\right)\right] \tag{3}$$

where the powers d_N were calculated[6] to be

$$d_N = \frac{4}{33-2N_f}\left[1 - \frac{2}{N(N+1)} + 4\sum_{j=2}^{N}\frac{1}{j}\right] \tag{4}$$

The predictions for flavor singlet structure functions are more complicated,[6] with two leading terms differing by less than one power of $\log Q^2/\Lambda^2$ in their asymptotic behavior as $Q^2 \to \infty$.

The results (1) to (4) are guaranteed[1,6,19] by the renormalization group to be the result of summing all the logarithms encountered in QCD perturbation theory. The moments (2) have the effect of picking out the matrix elements of operators of definite spin N[17] in the operator product expansion of two electromagnetic or weak moments. The power d_N is the anomalous dimension of scaling of the spin N operator. It results from exponentiation of the simple vertex corrections to the quark-antiquark operator indicated in Fig. 1a. The behaviors of the moments of singlet structure functions are more complicated because there are two operators of the same spin N, a two-gluon operator as well as a quark-antiquark operator, and they mix together through diagrams like that in Fig. 1b.

While the predictions (2) to (4) are precise, it is often convenient to reexpress them in terms of the evolution with Q^2 of the distribution of effective quark (or gluon) partons within the hadron target.[20] This can be done by inverting the expressions (3) and (4) for the moments $M_i(N,Q^2)$ by using a Mellin Transform.[21] The physics of the ensuing distributions $q(x,Q^2)$ (or $g(x,Q^2)$) can be seen very clearly from Fig. 1 when we recall that x is[4] the longitudinal momentum fraction carried by the parton. The anomalous dimensions d_N are

determined by the basic vertices of Fig. 2, which cause the parton distributions to evolve either by bremsstrahlung (Fig. 2a) or by pair creation (Fig. 2b). The equation controlling the evolution of $q(x,Q^2)$ at large Q^2 is just[22]

$$Q^2\frac{dq_i}{dQ^2}(x,Q^2) = \frac{\alpha_s(Q^2)}{2\pi}\int_x^1 dy\left[q_j(y,Q^2)P_{q_j\to q_i}\left(\frac{x}{y}\right)\right.$$
$$\left.+g(y,Q^2)P_{g\to q_i}\left(\frac{x}{y}\right)\right] \qquad (5)$$

and the evolution of $g(x,Q^2)$ obeys an analogous equation.[22] The "splitting" functions $P_{q\to q}$, $P_{g\to q}$, $P_{g\to g}$, $P_{q\to g}$ are easily calculable from the vertices of Fig. 2, and analogous to (for example) the equivalent photon distribution in Weiszäcker-Williams calculations in good old QED. As an example,[22]

$$P_{q_j\to q_i}(z) = \frac{4}{3}\delta_{ij}\left[\frac{1+z^2}{(1-z)_+} + \frac{3}{2}\delta(z-1)\right] \qquad (6)$$

and so on. The δ function in equation (6) just normalizes the fermion number to 1. The anomalous dimensions d_N can easily be reconstructed by taking the moments of equation (5), and are given by the z moments of the "splitting" functions like $P_{q\to q}$ in equation (6).

There are two reasons for focusing on the Q^2-dependent effective proton distributions $q(x,Q^2)$ and $g(x,Q^2)$. One reason is that they are the quantities directly related to the measured deep inelastic structure functions, and hence very convenient objects to work with phenomenologically. The other reason is that one might hope that they would have more universal applicability, and we will indeed see in the next section that recent theoretical calculations indicate that the same effective parton distributions can be used in many other phenomenological applications, such as in calculating hard quark-quark scattering contributions to large p_T hadron production, for example.

One can anticipate directly from the diagrams of Fig. 2 certain qualitative features[20] of the development of $q(x,Q^2)$ with increasing Q^2. Clearly both the bremsstrahlung and pair creation processes tend to degrade the parton longitudinal momenta as Q^2 is increased, and this can be seen directly by substituting the "splitting" function $P_{q\to q}(z)$ (6) into the evolution equation (5). Therefore deep inelastic structure functions will tend to fall in towards x=0 as $Q^2\to\infty$, in a manner indicated qualitatively in Fig. 3.[20] This behavior can also be seen in the form of the anomalous dimensions d_N (4). As $N\to\infty$, $d_N \propto \log N$, so that higher moments $M_i(N,Q^2)\to 0$ faster as $N\to\infty$. But the higher moments are seen from equation (2) to weight larger values of x closer to 1, and we see once more that the structure function at large x should fall to zero as $Q^2\to\infty$.

This trend is indeed seen in the data[23-25]: Figure 4 shows recent data from a FNAL muon scattering experiment, and superimposing data from different ranges of Q^2 clearly manifests the qualitative behavior that we anticipated in Fig. 3. On the other hand, almost any field theory would predict an analogous fall in towards x=0,[20]

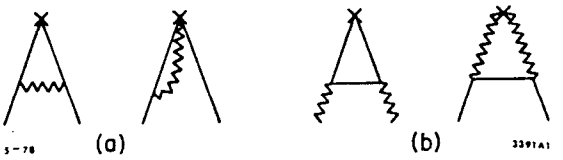

Fig. 1. Some diagrams contributing (a) to the anomalous dimensions of quark-antiquark operators, (b) to the mixing of flavor singlet operators.

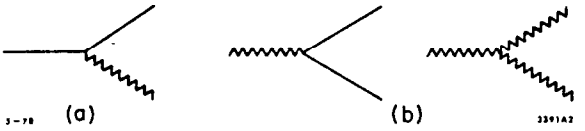

Fig. 2. The basic vertices for (a) gluon bremsstrahlung and (b) for $q-\bar{q}$ and gluon pair creation, which control the anomalous dimensions and the evolution of the quark and gluon distributions.

because basic vertices analogous to the bremsstrahlung and pair creation creation graphs of Fig. 2 exist in almost any field theory. What is specific to QCD is the characteristic logarithmic Q^2 dependence characterized by equations (1) to (4).

To compare these predictions with experimental data, several groups[26,27] have constructed parametrizations of effective quark and gluon distributions which are consistent with the QCD moment equations (2) to (4) (or equivalently the evolution equations (5) and (6)) and made phenomenological fits to the experimental data on eN, μN and νN scattering. Sample graphs from one such analysis[27] are displayed in Fig. 5: the fits seem to work at least semi-quantitatively. The particular graphs shown have been selected because they are the only ones made with a complete analysis[28] of the $O(1/\log Q^2/\Lambda^2$ and $\log\log Q^2/\log Q^2/\Lambda^2)$ correction terms in the moments (4), which arise from higher order terms in the evolution (1) of $\alpha_s(Q^2)$, in the anomalous dimensions, and in the matrix elements of the quark-antiquark operators. You see that the qualitative features of the fit are not greatly altered, so that one may conclude that QCD perturbation theory is reasonably convergent even at presently accessible values of Q^2. This reflects the fact $Q^2=O(5$ to $10)$ GeV^2 is already quite large on a hadronic scale, as expressed by the value $\Lambda\approx O(500)$ MeV found in typical analyses for the scale parameter Λ appearing in the logarithms (1) and (3) of asymptotic freedom. This sort of scale for the strong interactions means that the typical perturbation parameter $\frac{\alpha_s(Q^2)}{\pi}$ is comfortably small, being 0 (0.1 to 0.2)

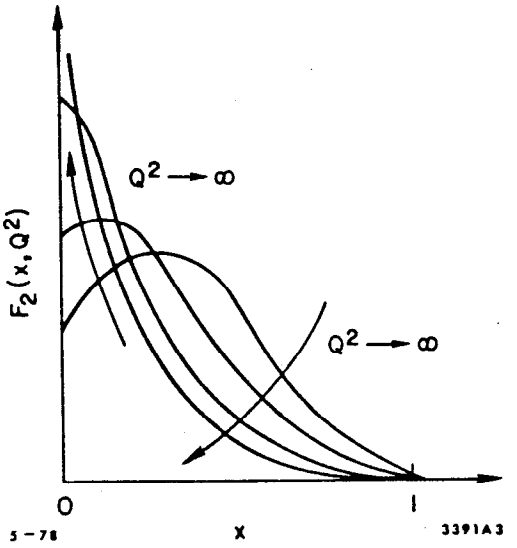

Fig. 3. Qualitative pattern of scaling violation in deep inelastic structure functions anticipated in QCD and other field theories.

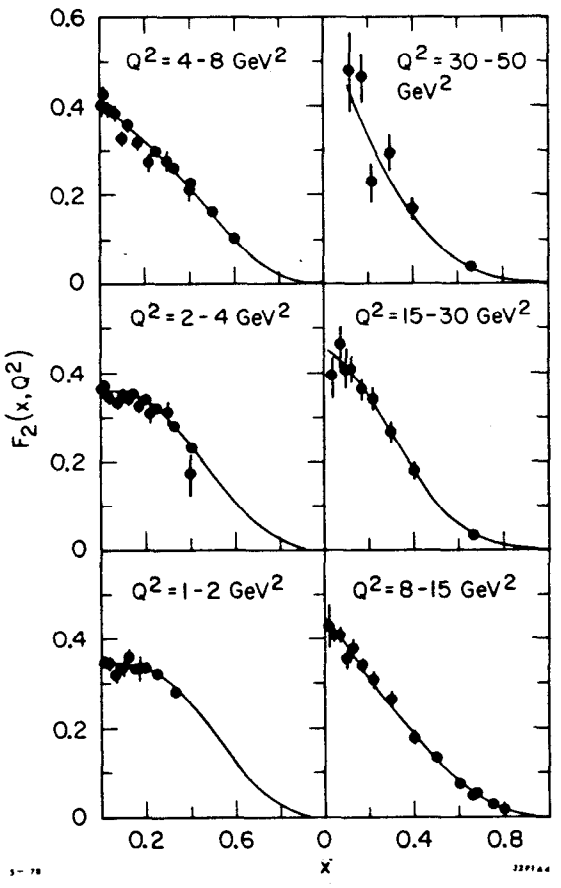

Fig. 4. Data from a FNAL[24] deep inelastic μ scattering experiment.

when Q^2=0 (5 to 10) GeV^2.

Although we see from Figs. 4 and 5 that QCD and asymptotic freedom fit the deep inelastic data qualitatively and semi-qualitatively, we would like some more precise numerical vindications of the predictions of the theory. In particular, we would like to have experimental confirmation of the gold-plated predictions (4) for the anomalous dimensions of QCD.[6] A preliminary analysis of just these parameters is now forthcoming from the BEBC group,[7] analyzing νN and $\bar{\nu}N$ charged current data both from their experiment at the CERN SPS and previous Gargamelle data from the CERN PS. They extract from their measured structure functions the moments of the structure functions F_2 and xF_3. One point of sophistication is that they use a modification[29] of the moments (2) which projects on to definite spin even at subasymptotic values of Q^2:

$$M_3(N,Q^2)\equiv\int_0^1 dx\ x^{N-2}\left[\frac{2}{1+\sqrt{1+\frac{4M^2x^2}{Q^2}}}\right]^{N+1} xF_3(x,Q^2)\left[\frac{1+(N+1)\left(1+\frac{4M^2x^2}{Q^2}\right)}{N+2}\right] \qquad (7)$$

In formula (7), M is the target nucleon mass, and the modifications to formula (4) just have the effect of removing trivial kinematic dependencies on the mass of the target. The first point to check is that the scaling violations seen in the moments of xF_3 are indeed consistent with the logarithmic Q^2 dependences expected from QCD. This they do by computing the quantities (Fig. 6)

$$\left[M_3(N,Q^2)\right]^{-1/d^N} \qquad (8)$$

which should be α log Q^2- log Λ^2. Graphs of the quantities (8) indeed indicate that they are approximately linear in log Q^2,[30] with the same intercept log Λ^2: $\Lambda\sim$700 MeV, at least for N=2,3,4 and 5. Power dependence in Q^2 with the ratios of anomalous dimensions found in lowest order for a vector gluon theory seems to give a significantly worse fit to the data. The linearity in log Q^2 and the common intercepts of the quantities (8) are non-trivial checks

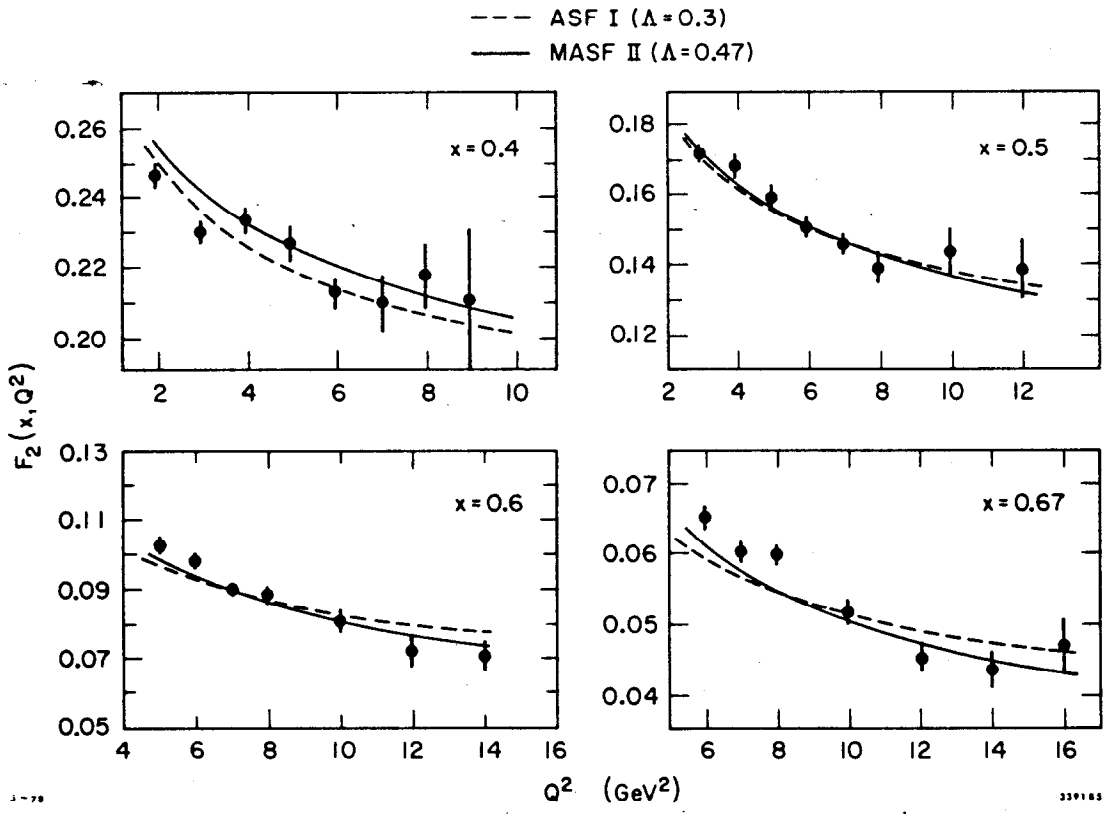

Fig. 5. Typical QCD fit to electroproduction[23] scaling violations, taken from Ref. 27.

of the QCD predictions (4). It is perhaps surprising that these properties hold all the way from Q^2=0(100) GeV^2 all the way down to Q^2=0(1) GeV^2, with no trace of subasymptotic effects due to higher twist operators[31] or quark mass effects.[32] You might also wonder what the effects should be of the higher order QCD perturbation theory effects[28] indicated schematically in equation (3). These have been evaluated by the BEBC group[7] using the results of Ref. 28, and turn out to cause modifications of the linear behaviors of the quantities (8) which are smaller than the present experimental errors for Q^2>0(1) GeV^2. Thus not only do the scaling violations (3) and (4) appear in the BEBC data, but also they are not clearly self-inconsistent.

The most convincing indication of the QCD predictions comes perhaps from comparing the Q^2 dependences of different moments $M_3(N,Q^2)$. Because of the expected asymptotic behaviors (3), the ratios

$$M_3(N,Q^2) \Big/ \left[M_3(N',Q^2)\right]^{dN/dN'} \tag{9}$$

should become constant as $Q^2 \to \infty$. Equivalently, if $\log M_3(N,Q^2)$ is plotted against $\log M_3(N',Q^2)$ one should see a straight line with slope dN/dN'. Figure 7 shows plots of different combinations of the $\log M_3(N,Q^2)$.[7] The solid lines are not fits to the data, but are lines with the slopes predicted by QCD - the agreement is rather

good, particularly when you recall that some of the moments vary with increasing Q^2 by about an order of magnitude. The following table[7] is a partial compilation of the best fit slopes on such straight line fits, compared with the theoretical predictions $d_N/d_{N'}$ of QCD. For comparison, the predictions of a model with scalar gluons[33] are also shown.

This remarkable agreement amounts to the first experimental check of unambiguous numbers predicted by QCD. It seems that the characteristic logarithms of QCD are indeed the dominant scale-breaking effects in the xF_3 structure function for Q^2 between 1 and 100 GeV^2. We might term this situation "precocious scaling violation".

In view of the successful comparison of theory and experiment in the xF_3 structure function, it is natural to ask about the F_2 structure function. Here the theoretical situation is more complex because of the new contributions[6] to scaling violations that were mentioned earlier, arising from gluons as well as quarks. It is possible to isolate[7] the gluon piece in QCD taking moments of F_2 and multiplying them by appropriately chosen (precisely specified)[7] functions of Q^2:

$$M_2(N,Q^2)\ Y(Q^2) = M_2(N,Q_o^2) + G(N,Q_o^2)\ X(Q^2) \qquad (10)$$

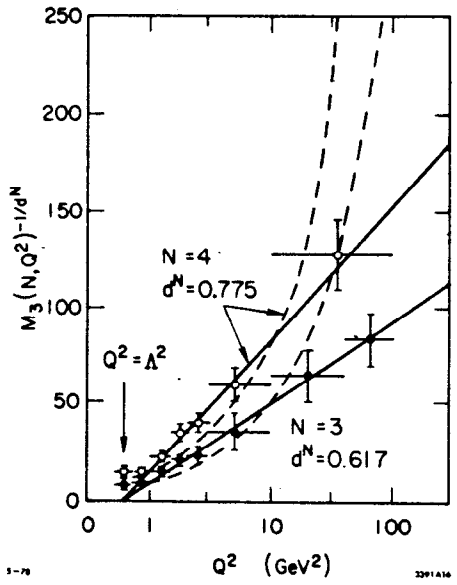

Fig. 6. Nachtmann[29] moments of xF_3, raised to the powers $(^{-1}/d_N)$.[7] QCD predicts an asymptotically linear dependence on log Q^2.

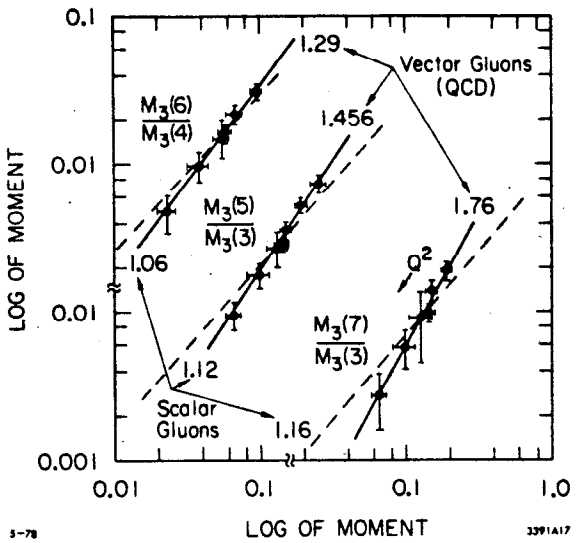

Fig. 7. Plots[7] of the logarithms of moments of xF_3. The solid lines have the slopes $d_N/d_{N'}$ predicted by QCD and other theories with vector gluons. The dashed lines have the slopes predicted by a scalar gluon theory[33] with a small fixed point coupling.

TABLE I

	d_5/d_3	d_7/d_3	d_6/d_2	d_6/d_4
QCD	1.46	1.76	2.53	1.29
Experiment	1.50±0.08	1.84±0.20	3.00±0.51	1.29±0.06
Scalar gluon model	1.12	1.16	1.43	1.06

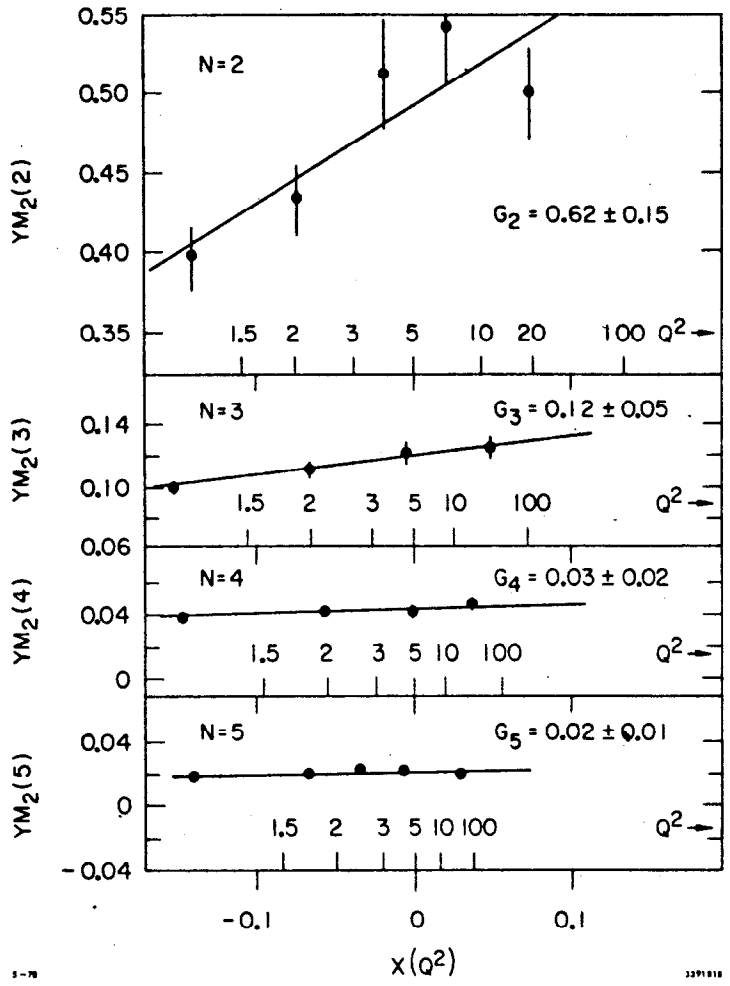

Fig. 8. Scaling violations[7] in the F_2 structure functions. The data would be independent of $X(Q^2)$ if there were no $q\bar{q}$ pair creation from gluons. The solid lines are QCD fits with the gluon moments indicated.

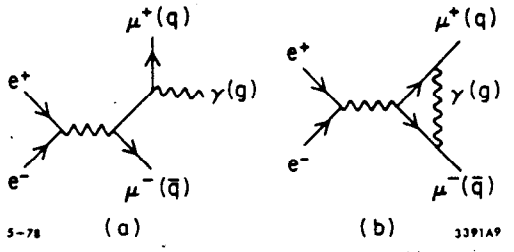

Fig. 9. Radiative corrections to $e^+e^- \to \mu^+\mu^-$ ($q\bar{q}$), (a) with a photon (gluon) in the final state, and (b) with virtual correction to the vertex.

where $G(N,Q_o^2)$ is the N'th moment of the effective gluon distribution $g(x,Q^2)$

$$Y(Q^2) \equiv X(Q^2) \equiv G(N,Q_o^2) = \int_o^1 dx\, x^{N-1} g(x,Q^2) \qquad (11)$$

Figure 8 plots a few of the quantities $M_2(N,Q^2)\ Y(Q^2)$ and indicates the clear need for the second, gluonic term on the right-hand side of equation (10). This term arises from quark-antiquark pair creation in the gluon field of the nucleon. The solid lines correspond to the gluons carrying $^0(_2)$ of the nucleon momentum at Q_o^2=4 GeV^2,[34] and having an x distribution similar to that of valence quarks. Clearly the data are consistent with these lines, but this analysis is not yet sufficiently advanced to constitute a conclusive test of QCD. A similar analysis of F_2 in deep inelastic eN and μN scattering, retaining all quark and gluon terms, has also been made,[35] with results for $G(2,Q^2)$ and $G(4,Q^2)$ which are compatible with the values used in Fig. 8.

The emerging picture is that not only are the qualitative trends of deep inelastic leptoproduction data[23-25] (see Fig. 4) compatible with QCD, but also semiquantitative QCD fits work very well[26,27] (see Figs. 5 and 8), and furthermore direct experimental quantitative confirmation of the anomalous dimensions predicted by QCD is now becoming available[7] (see Fig. 7 and the Table).[36] We await with interest the forthcoming results of analyses of large statistics CERN-SPS and FNAL νN and μN counter experiments.

3. OTHER APPLICATIONS OF QCD PERTURBATION THEORY

The successes of (renormalization group improved) QCD perturbation theory in the traditional applications to deep inelastic leptoproduction whet our appetite for more areas to apply the theory. There are other applications where the use of asymptotic freedom is underwritten by the renormalization group. But the most dramatic predictions, and the most rapid recent advances, may well lie in areas where the usual machinery of operator product expansions and the renormalization group is not directly relevant. The guiding principle has been that we cannot (yet) disentangle the infrared behavior of QCD, but we are able to study infrared behavior in perturbation theory.[37] The strategy is then to construct experimentally accessible quantities which avoid infrared singularities in perturbation theory, and not obviously vulnerable to incalculable non-perturbative effects. One tactic for doing this is to construct observables totally free of perturbative infrared singularities, such as jet cross-sections in e^+e^- annihilation.[9,38,39,40] Another tactic

is to identify a number of processes where the infrared singularities are universal and can be factored out,[41] leaving computable ultraviolet behavior to be compared with experiment. Examples are the Drell-Yan process hadron+hadron→$\ell^+\ell^-$+x,[42] large p_T hadron cross-sections in deep inelastic leptoproduction[43] and hadron-hadron collisions, and final state hadron distributions in leptoproduction and e^+e^- annihilation.[40,44] There follows a brief review of recently developed applications of QCD perturbation theory which adopt one or the other of these two tactics.

Jets in e^+e^- Annihilation

It has been known for a while that the infrared behavior of QCD perturbation theory is generally similar to that of QED.[37] For some time this was a cause for dejection, since it had been hoped that QCD perturbation theory would reveal significant clues to the quark confinement mechanism. But nowadays confinement is expected to be an essentially non-perturbative phenomenon.[12,13] Indeed, we are happy about the infrared similarities between QED and QCD perturbation theory, because they enable us to take over from QED many of the well-understood techniques for constructing quantities which are infrared finite in perturbation theory. In QED it is known[45] that if one introduces any of a range of dimensionless cut-offs - for example demanding that all except a fraction ε of the total center-of-mass energy in some process be emitted in two oppositely directed cones of center-of-mass opening angle δ - then there are no singularities when infrared regulators such as a photon (→gluon) or a lepton (→quark) mass are taken to zero.[46] As an example, consider the lowest order radiative corrections to $e^+e^-\to\mu^+\mu^-$ illustrated in Fig. 9. There are diagrams with real photons in the final state (Fig. 9a), as well as interferences between $e^+e^-\to\mu^+\mu^-$ diagrams with (Fig. 9b) and without virtual radiative corrections. The two classes of diagrams in Figs. 9a and 9b both have infrared singularities, but these cancel if one combines with the pure $\mu^+\mu^-$ final state "degenerate" final states[45] with either a "soft" photon with center-of-mass energy fraction $<\varepsilon$, or a "hard" photon emitted within a cone of angle δ of either the μ^+ or the μ^-. This QED procedure for defining infrared-finite cross-sections has a well-understood extension to all orders of perturbation theory.[45]

Now consider QCD perturbation theory for $e^+e^-\to$ hadrons. The lowest two orders are identical with QED, apart from trivial group-theoretical factors, so that the cancellation of infrared singularities will occur in the same way. Now one interprets[9] the cross-section for all except a fraction ε of the energy to be emitted within two cones of opening angle δ to be the cross-section for $e^+e^-\to$2 jets. The infrared finiteness of the 2-jet cross-section means that

$$\frac{\sigma_{2\text{ jet}}}{\sigma_{\text{total}}} = 1 - O\left(\frac{\alpha_s}{\pi}\right)$$

$$\frac{1}{\sigma_{\text{total}}}\frac{d\sigma(2\text{ jet})}{d(\cos\theta)} = \frac{3}{4}\left(1+\cos^2\theta\right) + O\left(\frac{\alpha_s}{\pi}\right) \qquad (12)$$

where the coefficients of α_s/π in equations (12) depend logarithmically on the dimensionless cut-offs ε and δ, and have recently been computed explicitly.[47] The results (12) hold in QCD perturbation theory, but an act of faith is still necessary to believe that these predictions are not invalidated by non-perturbative effects: perhaps those are connected with the finite p_T width of the jets actually observed[8] in e^+e^- annihilation and elsewhere.

If the infrared similarities between perturbation theory QCD and QED persist in higher orders, then not only two-jet but also multi-jet cross-sections should be predictable in QCD. Indeed, it has recently been shown that infrared singularities vanish for suitably defined multi-jet cross-sections.[48] The diagram of Fig. 9a for gluon bremsstrahlung at wide angles is an embryonic three-jet cross-section with a cross-section[9]

$$\frac{1}{\sigma_{\text{total}}} \frac{d^2\sigma(3\text{jets})}{dx_q\, dx_{\bar{q}}} = \frac{2\alpha_s}{3\pi} \left[\frac{x_q^2+x_{\bar{q}}^2}{(1-x_q)(1-x_{\bar{q}})}\right] + O\left(\frac{\alpha_s}{\pi}\right)^2 \qquad (13)$$

where x_q and $x_{\bar{q}}$ are the fractions of the center-of-mass energy Q carried by the quark and antiquark jets respectively: $x_q(\bar{q}) \equiv 2E_q(\bar{q})\text{jet}/Q$. We see from equation (13) that the gluon bremsstrahlung three-jet cross-section in the $e^+e^-\to$ hadrons continuum is expected to be $O(\alpha_s/\pi) \stackrel{?}{\sim} O(10)\%$. On the other hand, the dominant decay mode for a heavy 1^{--} quark-antiquark bound state such as the Υ is expected to be to three gluons.[49] Therefore one might expect that for sufficiently massive mesons three-jet final states should predominate,[38] with a cross section

$$\frac{1}{\Gamma_{\text{no }\gamma^*}} \frac{d^2\Gamma(3\text{jets})}{dx_1\, dx_2} = \frac{1}{\pi^2-9} \left[\frac{(1-x_1)^2}{x_2^2x_3^2} + \frac{(1-x_2)^2}{x_3^2x_1^2} + \frac{(1-x_3)^2}{x_1^2x_2^2}\right] + O\,\frac{\alpha_s}{\pi} \qquad (14)$$

It would certainly be very nice to verify experimentally the predictions (13) and (14). But how does one look for three-jet final states, particularly if they only constitute a small fraction of the total cross-section?

It has been pointed out[50] that there are directly computable experimental variables which should have distributions free of infrared singularities in QCD perturbation theory and hence be reliably (?) predictable. Final states with exceptional values of these variables should be fertile ground to search for multi-jet final states.[51] The trick is to find variables whose values are identical for the three configurations whose infrared singularities must cancel: a lone quark (Fig. 9b) or a quark and either a hard parallel or a soft gluon (Fig. 9a). Such variables will generally be linear in the momenta. One example is the "thrust" variable[50]

$$T \equiv \max\left[\frac{\sum_{\text{hadrons } h} |p_{\parallel}^h|}{Q}\right] \qquad (15)$$

where the maximization is performed with respect to the choice of a thrust axis for measuring $p_{\parallel}$. A final state with $T \simeq 1$ will have

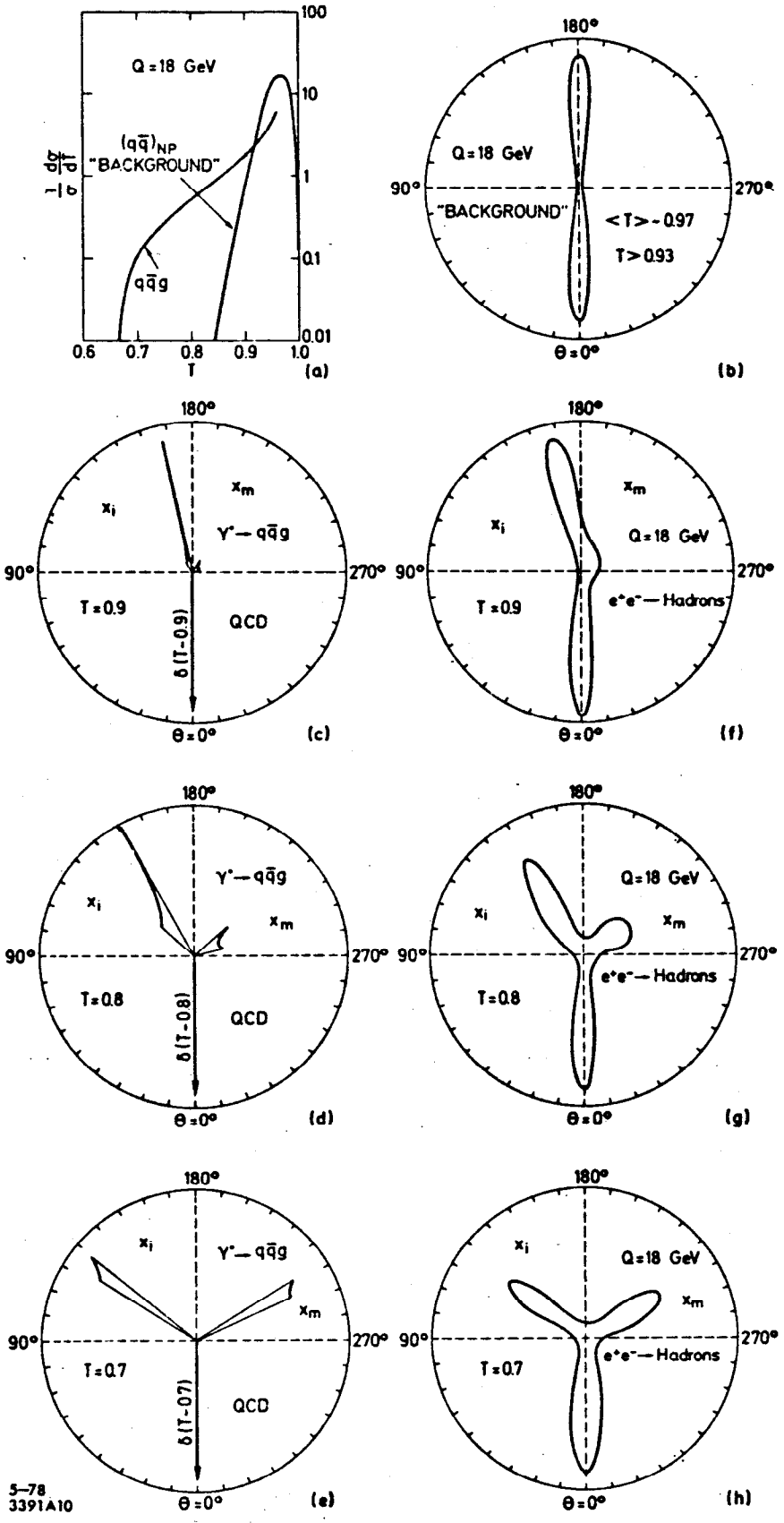

Fig. 10. (a) Comparison[40] of the thrust distribution from QCD perturbation theory with an estimate of the non-perturbative smearing of two-jet configurations (b) at a center-of-mass energy Q=18 GeV, and (c), (d), (e) distributions of the hadron energy (Pointing vector) in the event plane computed in QCD, smeared (f), (g) and (h) by non-perturbative effects.

hadrons with highly collimated momenta, and the final state will have two jets. Events with low thrust T<1 should mostly have a three-jet structure. The putative multi-jet cross-sections (13) and (14) correspond to thrust distributions

$$\frac{1}{\sigma_{\text{total}}}\frac{d\sigma}{dT} \approx \frac{2\alpha_s}{3\pi}\left[\frac{2(3T^2-3T+2)}{T(1-T)}\ln\frac{2T-1}{1-T} - \frac{3(3T-2)(2-T)}{(1-T)}\right] \qquad (16)$$

and

$$\frac{1}{\Gamma_{\text{no }\gamma^*}}\frac{d\Gamma}{dT} \approx \frac{3}{\pi^2-9}\left[\frac{4(1-T)}{T^2(2-T)^3}(5T^2-12T+8)\ln\frac{2-2T}{T} + \frac{2(3T-2)(2-T^2)}{T^3(2-T)^2}\right] \qquad (17)$$

which are plotted in Figures 10a and 11a respectively. If we select an event with low T, perturbation theory would predict that it be approximately planar. If we plot the angular distribution of the radiated hadronic energy projected on to the event plane (the "Pointing Vector"[40]), then for low T events it should have an angular distribution characteristic of three-jet structures. The results corresponding to (13) and (14), computed with a model for the finite non-perturbative p_T spread of each jet, are shown in Figures 10b to h and 11b to h for the e^+e^- continuum and for T decay respectively. If QCD perturbation theory predictions for multi-jet cross-sections are indeed reliable as we believe,[48] then there should be many interesting hadronic final states in e^+e^- annihilation. Similar infrared finite jet predictions can be made for eN, μN, νN and hadron-hadron collisions, but calculating them requires more understanding of infrared singularities associated with individual hadrons in the initial or final state, which we now discuss.

Factorizing Infrared Singularities

Up to now we have permitted our ignorance of the infrared behavior of QCD to restrict ourselves to calculating quantities which have no infrared singularities. But we can relax this criterion by identifying classes of "hard" processes involving large momentum transfers where universal infrared singularities factorize out.[11,41] We can then study ratios of these cross-sections which are only sensitive to the calculable ultraviolet properties of the theory. To see how this program should work, let us contemplate the generic "hard scattering" process illustrated in Fig. 12: a certain number of large Q^2 currents (virtual photons or W bosons?) interact with constituents from a collection of hadrons, of which some are in the initial and some in the final state. We presume that the constituents a, b,... of the hadrons A, B,... have finite (momentum)^2 p_a^2, p_b^2, ..., while the (momentum)^2 Q_i^2 of the currents, and all the momentum transfers between different active participants in the "hard" process all $\to\infty$ in constant ratios. Suppose we calculate in QCD perturbation theory using a coupling constant renormalized at some large momentum Q_0^2: $\alpha_s(Q_0^2)$. Then we will encounter logarithms in the relevant Feynman diagrams which are of two types: $\ln(Q^2/Q_0^2)$ (to be called ultraviolet), and $\ln(Q^2/p_{a,b,\ldots}^2)$ (to be called infrared).

Fig. 11. Similar to Fig. 10, computed[40] for $T \to 3$ gluons.

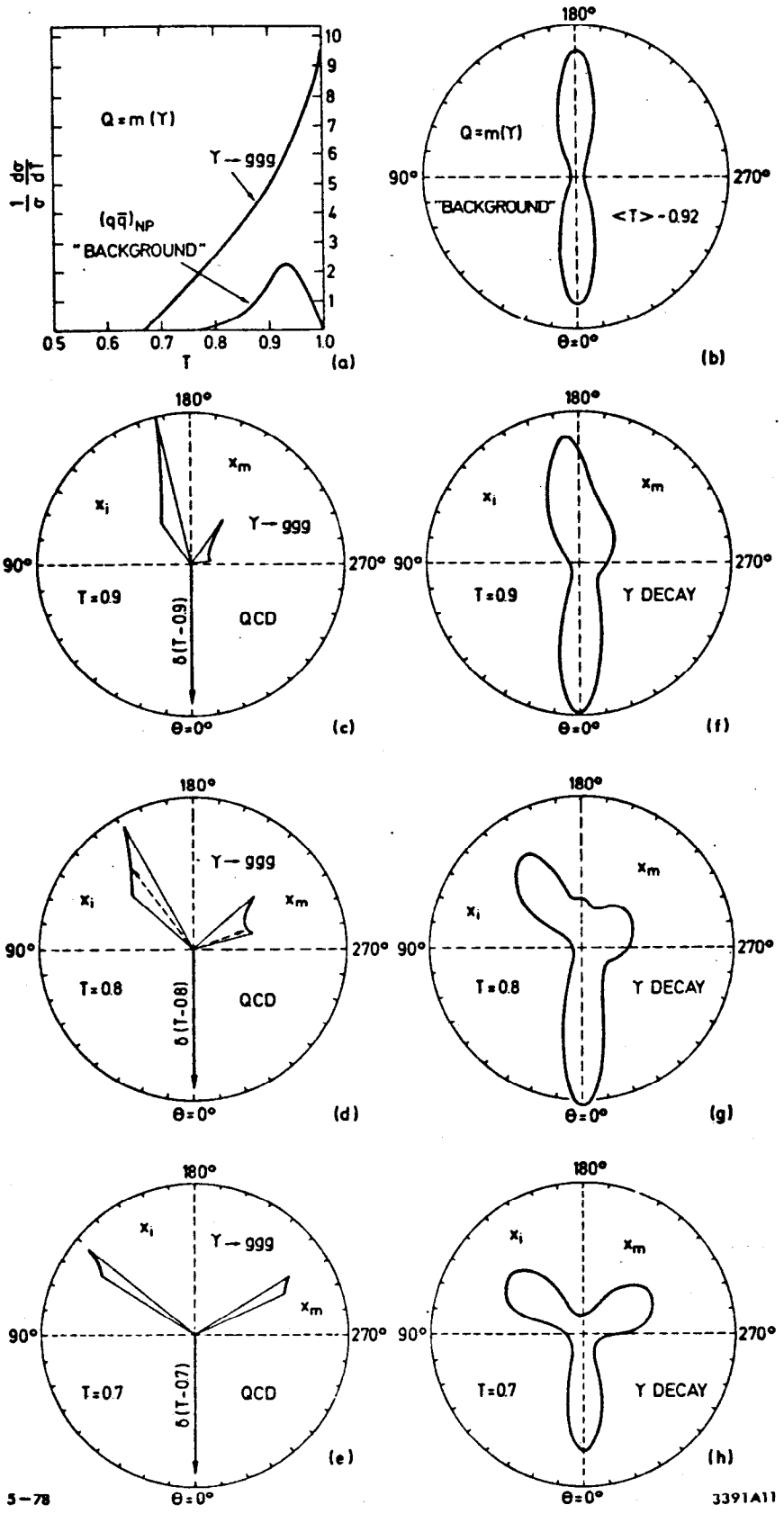

The only dependence on the bound state properties resides in the infrared logarithms, and the hope is that this dependence factorizes[11,41] into separate universal terms for each external hadronic leg[52]:

$$\sigma \approx \sigma_{Hard}(\alpha_s(Q_0^2), \ln Q^2/Q_0^2) \times \prod_{A,B,\ldots}^{\pi} F_{Aa}(\alpha_s(Q_0^2), \ln Q^2/Q_0^2, \ln Q^2/p_a^2) \quad (18)$$

The ultraviolet logarithms will then arrange themselves so that the cross-section can be re-expressed in terms of the coupling constant at Q^2: $\alpha_s(Q^2)$, and one can then rewrite

$$\sigma \approx \sigma_{Hard}(\alpha_s(Q^2)) \times \prod_{A,B,\ldots}^{\pi} F_{Aa}(Q^2)$$

where σ_{Hard} will be given in leading order by the Born terms. The universal distribution functions $F_{Aa}(Q^2)$ will be the same in different scattering processes. In particular, those connected with initial state hadrons will be the same as in deep inelastic leptoproduction,[41] and so should be identified as the effective quark and gluon distributions introduced earlier and obeying[22] equations like (5). If there is also factorization of the infrared logarithms relating to final state hadrons,[11] then one would also have universal quark (or gluon)→hadron fragmentation functions, which would play roles analogous to those in the naive parton model,[4] albeit with scaling violations analogous to those for the initial distribution functions (cf equations (2) to (5)). If we want, we may sum over all hadrons emanating from one of the final state constituents, in which case we expect to cancel the associated infrared singularities and arrive at an infrared finite and hence calculable jet cross-section.

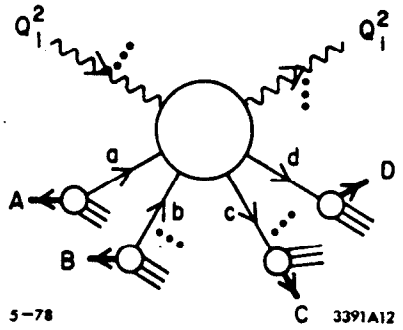

Fig. 12. A generic hard scattering diagram with deep inelastic currents Q_1^2 to Q_1^2, and constituents a, b, c and d of hadrons A, B, C and D. All momentum transfers and Q^2 are supposed large.

To what "hard" scattering reactions can this approach be applied, and what calculations have been done to support the factorization picture outlined above? If we first look at the total electroproduction cross-section ep→e+x illustrated in Fig. 13 then the derived

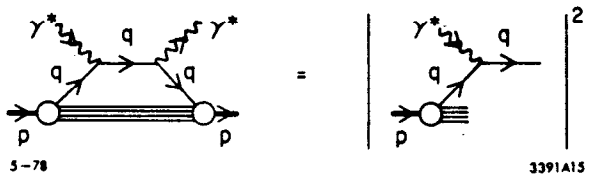

Fig. 13. A sample "hard" scattering cross-section: the total electroproduction cross-section is the modulus squared of the hard subprocess γ*+q→q, folded with the distribution $q(x,Q^2)$ of quarks in the proton.

factorization is guaranteed by the renormalization group.[1,41] It tells us that the development of the structure function at large Q^2

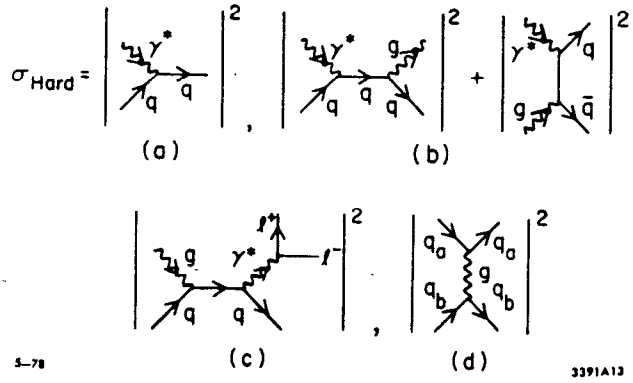

Fig. 14. Hard subprocesses relevant to (a) the electroproduction cross-section, (b) large p_T production in electroproduction; (c) Drell-Yan pair production at large p_T and (d) large p_T production in hadron-hadron collisions.

is controlled by the anomalous dimensions (4), or equivalently the evolution equation (5). The Born term for σ_{Hard} in equation (19) is just the point-like charge coupling of Fig. 14a. The infrared sensitivity resides in the boundary conditions to be fed into the evolution equation (5). When the leading logarithms in $e^+e^- \rightarrow$ hadron C+x are studied,[11,43,53] they are also found to exhibit the desired factorization, with the point-like Born term of Fig. 14a and an infrared sensitive quark→hadron fragmentation function $F_{C\rightarrow C}(Z,Q^2)$, where $Z \equiv E_C/E_C$. The high Q^2 development of $F_{C\rightarrow C}$ is controlled by anomalous dimensions and an evolution equation which is just the analytic continuation of equation (5), and reflects the same physical processes of bremsstrahlung and pair creation. (Notice though that the initial conditions for these evolution equations are infrared sensitive and not related by analytic continuation.) The factorization property becomes very important when it is demonstrated and used for $e+p\rightarrow e+C+x$, because it means that a simple partonesque[4] "building block" formula applies to the cross-section for producing final state particles with longitudinal momentum fraction Z at low p_T:

$$\sigma(e+p\rightarrow e+C+x = \sum_{q,\bar{q}} q(x,Q^2)e_q^2 F_{q\rightarrow C}(Z,Q^2) \qquad (20)$$

A non-partonesque[4] process is the production of large p_T jets in electroproduction.[43] Here the lowest order hard process is wide angle "Compton scattering" $\gamma^*+q\rightarrow g+q$ (or pair production $\gamma^*+g\rightarrow q+\bar{q}$) as in Fig. 14b, and if the factorization property holds the only infrared singularities are those connected with the target proton, which are the same as in the total electroproduction cross-section, so that one may write

$$\sigma_{\text{large } p_T \text{ jets}} = \sum_{q,\bar{q}} q(x,Q^2)\sigma(\gamma^*+q\rightarrow g+Q))\Big|_{\alpha_s(Q^2)} + \begin{matrix}\text{gluon}\\ \text{terms}\end{matrix} \qquad (21)$$

Of course one may always study the production of individual final state hadrons at large p_T, in which case formula (21) is just convoluted with the same fragmentation function $F_{q\rightarrow C}(Z,Q^2)$ as appeared in equation (20). And so it goes.

So far we have not considered processes with two initial state hadrons: the simplest such reaction is the Drell-Yan process $pp\rightarrow \ell^+\ell^-+x$. Here again, infrared factorization[42] has been demonstrated[53] to all orders at the leading logarithm level, meaning that the naive

Fig. 15. The single fermion loop calculated[14] in the presence of a background instanton field of size ρ located at the point z.

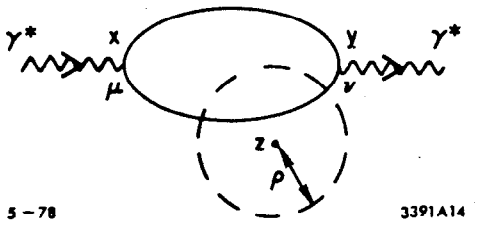

QCD modification of the usual parton cross-section formula is indicated:

$$M^4\frac{d\sigma}{dM^2} = \frac{4\pi\alpha^2}{9}\sum_{q\bar{q}}\int_0^1 dx_q \int_0^1 dx_{\bar{q}}\, e_q^2\, q(x_q, M^2)\bar{q}(x_{\bar{q}}, M^2)\delta(x_q x_{\bar{q}} - M^2/s) + O(\alpha_s/\pi) \qquad (22)$$

There are however some important QCD corrections to the usual parton physics of this reaction. First, the essential scale invariance of QCD at short distances means that there is no p_T cut-off, and therefore the average p_T^2 of the lepton pair should grow $\propto M^2$ (to within logarithms). Care should be taken in comparing this prediction with existing data, since $\langle p_T^2 \rangle$ may also depend on the value of $\tau \equiv M^2/s$ being studied.[54] The dependence on M^2 and τ should be carefully disentangled when comparing theory and experiment, but the growth with M^2 at fixed τ does seem to be present in the data. Another important remark concerns the $O(\alpha s/\pi)$ pieces in equation (22): the basic $O(\alpha s/\pi)^0$ $q\bar{q}$ annihilation piece may be rather small in pp collisions, just because the proton contains relatively few antiquarks. Rival hard subprocesses which are naively suppressed by $O(\alpha s/\pi)$ such as $g+q\to(\ell^+\ell^-)+q$ (see Fig. 14c), or even $O(\alpha s/\pi)^2$ like $q+q\to(\ell^+\ell^-)+q+q$, may also be just as important phenomenologically.[55] The Drell-Yan process is probably rather free of these problems in πp or $\bar{p}p$ collisions: their significance for the total $pp\to(\ell^+\ell^-)+x$ cross-section has not yet been fully calculated.

The final "hard" process we should mention is pp→large p_T hadrons + x. This process is interesting because it may constitute the first theoretically "clean" testing-ground for QCD in pure hadronic collisions. The required factorization of all initial- and final-state infrared logarithms has been verified for the leading logarithms in the lowest non-trivial order of perturbation theory,[56] and arguments exist that this factorization persists in higher orders.[57] If so, this means that at very large transverse momenta the correct QCD prescription for the quark-quark cross-section of Fig. 13d is

$$E_c\frac{d\sigma}{d^3p_c}(A+B\to C+x) = \sum_{a,b,c,d}\int_0^1 dx_a \int_0^1 dx_b \int_0^1 \frac{dx_c}{x_c^2} \times \left[q_a(x_a,s')q_b(x_b,s')F_{c\to C}(x_c,s')\right] \times \delta(s'+t'+u')\,\frac{s'}{\pi}\frac{d\sigma}{dt'}(q_a+q_b\to q_c+q_d)\Big|_{\alpha_s(s')} + \ldots \qquad (23)$$

where the dots comprise the "hard" scattering of other types of constituent, terms of higher order in α_s/π, and so on. The QCD large p_T formula (23) has many sources of scaling violation, and its application is complicated by the non-zero p_T of the initial-state constituents. The writer is no expert on large p_T phenomenology, but it does seem possible that some fraction of present large p_T data may indeed result from the fundamental "hard" scattering diagrams of QCD.

Recent theoretical progress has made available many predictions of QCD perturbation theory for "hard" processes beyond the traditional applications of Section 2 which were guaranteed by operator product expansions and the renormalization group. It would be important to find a comparably reliable and general theorem to underpin these new applications of QCD perturbation theory, but already they look to be reliable predictions eager to be confronted with experiment.

4. NON-PERTURBATIVE EFFECTS AT LARGE MOMENTA

So far we have concentrated on results which hold in perturbation theory in QCD. But we believe that non-perturbative effects[12] have some very important phenomenological consequences, such as quark confinement.[13] We should ask whether non-perturbative effects are also important at large momenta, where we have made our applications of QCD perturbation theory so far. The normal procedure for studying non-perturbative phenomena is to use the functional integral and construct semi-classical approximations to it. The WKB approach first looks for solutions of the classical Euclidean field equations,[12] which correspond to minima of the action and hence stationary points of the functional integrand. One then does perturbation theory around each classical solution, adds them together weighted by the classical Euclidean actions e^{-A}, and finally continues amplitudes back to Minkowski space.[58] This procedure is incomplete, in that there may be other non-perturbative configurations with larger actions, which nevertheless occur in large enough numbers (entropy) to overcome the exponential suppressions of their e^{-A} factors.[13] As a starting point we ignore this complication and concentrate on the classical extrema, which are known in the case of QCD to be multi-instanton (-anti-instanton) configurations.[12] The action of a single instanton is known to be

$$A = \frac{8\pi^2}{g^2} \tag{24}$$

where one-loop perturbative calculations[59] in the presence of an instanton indicate that g^2 in equation (24) is to be interpreted as $g^2(\rho)$ (of equation (1) with $Q^2 \approx \frac{1}{\rho^2}$), where ρ is the usual size parameter of the instanton. Asymptotic freedom (1) means that $A \to \infty$ when the size $\rho \to 0$, so that small instantons make relatively small contributions to the functional integral. We might hope that processes at large Q^2 would somehow only "feel" small instantons of size $\rho \sim 1/Q$, in which case the weighing of e^{-A} and equations (1) and (24) would suggest that non-perturbative effects would fall like a power of Q^2 as $Q^2 \to \infty$.

Some calculations to explore this possibility have been done

recently[14]: what has been studied is the contribution of the simplest non-trivial non-perturbative configuration (one instanton) to the most basic short distance or deep inelastic process ($e^+e^-\to$hadrons at high Q^2), evaluating the lowest order Feynman diagram (the simple fermion loop of Fig. 14). If the contribution to $\sigma(e^+e^-\to\text{hadrons})$ at large Q^2 were dominated by small instantons, then this calculation could be regarded as the leading term of a non-perturbative calculation in the conventional "dilute gas approximation"[13] in which instantons (and anti-instantons) are supposed to be non-interacting and not very dense.

It does indeed turn out that this one-instanton contribution to $R\equiv\sigma(e^+e^-\to\text{hadrons})/\sigma(e^+e^-\to\mu^+\mu^-)$ is controlled by such small instantons of size $\rho=0(1/Q)$. The fermion loop of Fig. 13 is easily calculated[14] using the known[60] fermion propagator $S^1(x,y;z,\rho;m)$ in the presence of an instanton located at z and of size $\rho>>1/m$:

$$\delta\pi_{\mu\nu}(x,y)\equiv\langle 0|T(J_\mu(x)J_\nu(y))|0\rangle_{\text{instanton}} = \int d^4z_\mu \int_0^\infty d\rho\, d(\rho)$$
$$\Big[-\mathrm{Tr}(\gamma_\mu S^1(x,y;z,\rho;m)\gamma_\nu S^1(y,x;z,\rho;m)) + \mathrm{Tr}(\gamma_\mu S^0(x,y;m)\gamma_\nu S^0(y,x;m))\Big] \tag{25}$$

The density function $d(\rho)$ for the instantons is known from the work

$$d(\rho) = \frac{0.1}{\rho^5}\left(\prod_{i=1}^{N_F} m_i\right)(1.3\ \Lambda\rho)^{N_f}\exp\left(\frac{-8\pi^2}{g^2(\rho)}\right)\left(\frac{8\pi^2}{g^2(\rho)}\right)^6 \tag{26}$$

Transforming equation (25) to momentum space one finds

$$\delta\Pi^\mu_\mu(Q) = \int_0^\infty d\rho\, d(\rho)\left[\frac{-12}{Q^2} + 36\rho^2\int_0^1 dx K_2\left(\frac{2\rho Q}{\sqrt{1-u^2}}\right)\right] \tag{27}$$

The first term in equation (27) gives a contribution to the real part of the vacuum polarization which is suppressed by $0(1/Q^4\ln Q^2)$ relative to the leading perturbative contribution.[14] However its (singular) contribution to the absorptive part relevant to R is cancelled by the singularity in the second term at $Q^2=0$. The only contribution to the instanton piece (27) explicitly comes[14] from $\rho=0(1/Q)$, and yields

$$\frac{\Delta R}{R}\underset{\substack{Q\to\infty\\ N_f\neq 3,9,\ldots}}{\approx}\left(\frac{Q}{\Lambda}\right)^{-11-N_f/3}\left(\ln Q^2\right)^{6\left(\frac{33-4N_f}{33-2N_f}\right)}\times 6\pi^{3/2}(0.1)(1.3)^{N_f}\frac{33-2N_f}{6}^6\cos\frac{\pi N_f}{6}$$
$$\times\frac{\Gamma\left(\frac{7}{2}+\frac{N_f}{6}\right)\times\left[\Gamma\left(\frac{11}{2}+\frac{N_f}{6}\right)\right]^2}{\Gamma\left(6+\frac{N_f}{6}\right)}\left(\frac{\prod_{i=1}^{N_f}\bar{m}_i}{\Lambda^{N_f}}\right) \tag{28}$$

with a related form[14] for $N_f = 3,9,\ldots$

A numerical evaluation relevant between the strangeness and charm threshold yields

$$\frac{\Delta R}{R} \approx \left(\frac{Q}{1{\cdot}5\ \text{GeV}}\right)^{-12} (\ln Q^2)^{3{\cdot}67} \tag{29}$$

if $\Lambda \sim 500$ MeV. The detailed form and value of ΔR (28) and (29) are probably phenomenologically meaningless and undetectable, but they indicate that in e^+e^- annihilation there is probably some sort of non-perturbative "brick wall" somewhere between 1 and 2 GeV in the center-of-mass. Above this point QCD perturbation theory probably reigns supreme, whereas at lower energies non-perturbative effects are O(1). It is encouraging that this is just the region where vector meson resonances are known to lie.

It is interesting that this simplest possible calculation supports the "non-perturbative perturbation theory" picture we hoped to find. But many more calculations are needed of more complex diagrams for more complicated processes in the presence of more intricate background fields before we can feel sure that non-perturbative phenomena are always small at large Q^2. Nevertheless, we may legitimately hope that non-perturbative effects will not invalidate the elegant pattern of perturbative QCD predictions that we discussed in Sections 2 and 3.

5. CONCLUSIONS AND QUESTIONS

On the basis of the previous discussion, the following seem reasonable conclusions about the status of phenomenological applications of QCD:

The classic asymptotic freedom predictions of renormalization group improved QCD perturbation theory for deep inelastic leptoproduction triumphantly pass present tests. In addition to the familiar qualitative successes of QCD fits to deep inelastic scaling violations, we now find for the first time that the anomalous dimensions predicted by QCD are receiving direct experimental confirmation. We look forward to detailed analyses of the large statistics νN and μN experiments which should be available soon. In particular we may hope for analyses of the flavor singlet structure functions which are as striking as the BEBC analysis[7] of the xF_3 structure function.

Recent theoretical work suggests that there are many other high momentum transfer processes where QCD perturbation theory can legitimately be applied to make reliable predictions. These include jet production, final state hadron distributions in deep inelastic processes at small and large p_T, Drell-Yan lepton pair production and hadron-hadron collisions at large p_T. We look forward to experimental tests of these predictions.

Finally, we see reason to hope that non-perturbative QCD effects may not invalidate the predictions of QCD perturbation theory that we have been discussing. Unfortunately, the other side of this coin is that a convincingly calculable and testable phenomenological manifestation of non-perturbative QCD has yet to be identified.

This is just one of many open questions about applications of

QCD. A partial list might include: How can we be sure the strong coupling constant is really asymptotically free? Many of the tests of Section 2 would be successful if there was a fixed point reasonably close to the origin, so that moments violated scaling by small powers of Q^2 instead of log Q^2. Presumably we should do experiments at much higher Q^2, using for example[30] high energy electron-proton colliding rings? What about σ_L/σ_T, where experimental results are not in dramatic agreement with experiment?

Presently observed jets seem to have a finite p_T cut-off. Can we understand this, or (which may be equivalent) be sure that non-perturbative effects really don't mess up our perturbative jet predictions? Can we say something about the hadronic wavefunctions or fragmentation functions? At the moment we just factor out our ignorance about them. Although we have not discussed them here, heavy quark-onium states seem particularly amenable to perturbative analysis, but we are still short on rigorous theoretical understanding.

Finally, can we find some unambiguous and calculable physical manifestation of the non-perturbative QCD phenomena now being intensively studied? We hope ultimately to be able to calculate the hadron spectrum, but in the meantime is there any way of "seeing" an instanton? Or a meron?

There are still more open questions than closed solutions.

ACKNOWLEDGMENTS

It is a pleasure to thank J.D. Bjorken, S.J. Brodsky and R.C. Brower for useful comments and discussions, and S.D. Drell for the hospitality of the SLAC theory group.

REFERENCES AND FOOTNOTES

1. For general reviews of QCD, see H.D. Politzer, Phys. Reports 14C, 129 (1974); W. Marciano and H. Pagels, Phys. Reports 36C, 137 (1977).
2. D.J. Gross and F.A. Wilczek, Phys. Rev. Lett. 30, 1343 (1973); H.D. Politzer, Phys. Rev. Lett. 30, 1346 (1973).
3. T. Applequist and H.D. Politzer, Phys. Rev. Lett. 34, 43 (1975) and Phys. Rev. D12, 1404 (1975). For a recent phenomenological review and references see K. Gottfried, Proceedings of the 1977 International Symposium on Lepton and Photon Interactions at High Energies, ed. F. Gutbrod, (DESY, 1977) p. 667.
4. J.D. Bjorken and E.A. Paschos, Phys. Rev. 158, 1975 (1969); S.D. Drell, D.J. Levy and T.-M. Yan, Phys. Rev. D1, 1035 (1970); R.P. Feynman, "Photon-Hadron Interactions" (Benjamin, New York, 1972).
5. S. Okubo, Phys. Lett. 5, 165 (1963); G. Zweig, CERN preprints TH 401, 412 (1964); J. Iizuka, Suppl. Progr. Theor. Phys. 37-38, 21 (1966). For other discussions of QCD and "soft" hadronic processes, see G. Veneziano, Nucl. Phys. B117, 519 (1976) and references therein.
6. D.J. Gross and F.A. Wilczek, Phys. Rev. D8, 3633 (1973) and D9, 980 (1974); H. Georgi and H.D. Politzer, Phys. Rev. D9, 416 (1974).

7. P.C. Bosetti et al., CERN preprint "Analysis of Nucleon Structure Functions in CERN Bubble Chamber Neutrino Experiments" (1978). For a preliminary analysis, see K. Schultze, Proceedings of the 1977 International Symposium on Lepton and Photon Interactions at High Energies, Hamburg, ed. F. Gutbrod (DESY, 1977), p. 359. I thank Bill Scott for useful discussions about the analysis.
8. G. Hanson et al., Phys. Rev. Lett. 35, 1609 (1975).
9. For an early theoretical discussion of jets, see A.M. Polyakov, Soviet Phys. JETP 32, 296 (1971); 33, 850 (1971). For the more recent application to QCD, see J. Ellis, M.K. Gaillard and G.G. Ross, Nucl. Phys. B111, 253 (1976); G. Sterman and S. Weinberg, Phys. Rev. Lett. 39, 1436 (1977).
10. S.D. Drell and T.-M. Yan, Phys. Rev. Lett. 25, 316 (1970). For the most complete analysis in QCD perturbation theory see Yu. L. Dokshitzer, D.I. D'yakonov and S.I. Troyan, Materials for the XIIIth Leningrad Winter School (1978), p. 3 and Leningrad Nuclear Physics Institute preprint "Hard Semi-inclusive Processes in QCD" (1978).
11. For early discussions see A. Mueller, Phys. Rev. D9, 963 (1974); C. Callan and M. Goldberger, Phys. Rev. D11, 1553 (1975). There is a heuristic review by A.M. Polyakov, Proceedings of the 1975 International Symposium on Lepton and Photon Interactions at High Energies, Stanford, ed. W.T. Kirk (SLAC, 1975) p. 855. For a discussion in the context of QCD see H. Georgi and H.D. Politzer, Harvard University preprint HUTP-77/A071 (CALT-68-629) (1977).
12. A.A. Belavin, A.M. Polyakov, A.S. Schwartz and Yu.S. Tyupkin, Phys. Lett. 59B, 85 (1975). For a complete review, see S. Coleman, Harvard University preprint HUTP-78/A004 (1978).
13. A.M. Polyakov, Nucl. Phys. B121, 429 (1977); C. Callan, R. Dashen and D.J. Gross, Princeton Institute for Advanced Study preprint C00-2220-115 (1977).
14. N. Andrei and D.J. Gross, Princeton University preprint "The Effect of Instantons on the Short Distance Structure of Hadronic Currents" (1978); R.D. Carlitz and C. Lee, Pittsburgh University preprint PITT-193 (1978); L. Baulieu, J. Ellis, M.K. Gaillard and W.J. Zakrzewski, CERN preprint TH 2482 (1978).
15. Although few theorists would seriously question the necessity of discussing non-perturbative phenomena in QCD, and believe that the functional integral is the correct framework for studying them, I am unaware of any unassailable theoretical or phenomenological proof that they must be incorporated in the fashion of references 12, 13 and 14. This makes non-perturbative effects all the more fascinating.
16. N_f is the number of quark flavors which have masses $m_i \ll Q$, and so can be presumed to have "switched on" at the momenta of interest. See H. Georgi and H.D. Politzer, Phys. Rev. D14, 1829 (1976). Λ is a mass parameter setting the scale of the strong interactions which is arbitrary a priori, but generally expected to be O(300 MeV to 1 GeV).
17. J.M. Cornwall and R.E. Norton, Phys. Rev. 177, 2584 (1969). The variable x is the conventional Bjorken scaling variable $x=Q^2/2\nu$.

Asymptotically at large Q^2 these moments project on to channels with definite spin N in the crossed channel. There are modifications to the Cornwall-Norton moments which make precise spin projections at finite Q^2: see equation (7) and reference 29.

18. For a negative search for asymptotic freedom in non-gauge theories, see S. Coleman and D.J. Gross, Phys. Rev. Lett. 31, 851 (1973); though it is possible to construct implausible spontaneously broken gauge theories with asymptotic freedom. The renormalization group says that theories with ultraviolet fixed points away from the origin will violating scaling by powers of Q^2: K.G. Wilson, Phys. Rev. 179, 1499 (1969).
19. N. Christ, B. Hasslacher and A. Mueller, Phys. Rev. D6, 3543 (1972).
20. For a very physical discussion, see J. Kogut and L. Susskind, Phys. Rev. D9, 697 and 3391 (1974).
21. G. Parisi, Phys. Lett. 43B, 207 (1973); D.J. Gross, Phys. Rev. Lett. 32, 1071 (1974).
22. G. Altarelli and G. Parisi, Nucl. Phys. B126, 298 (1977).
23. R.E. Taylor, Proceedings of the 1975 International Symposium on Lepton and Photon Interactions at High Energies, Stanford, ed. W.T. Kirk (SLAC, 1975) p. 679; E.M. Riordan et al., SLAC preprint PUB-1634 (1975).
24. L.N. Hand, Proceedings of the 1977 International Symposium on Lepton and Photon Interactions at High Energies, Hamburg, ed. F. Gutbrod (DESY, 1977) p. 417. The data shown here come from the Chicago-Harvard-Illinois-Oxford group, courtesy of T.W. Quirk.
25. For some published data see ref. 7 and T.H. Burnett, Proceedings of the 1977 International Symposium on Lepton and Photon Interactions at High Energies, Hamburg, ed. F. Gutbrod (DESY, 1977) p. 227. Similar trends are apparent in the data of the CDHS counter experiment at CERN.
26. For a review see O. Nachtmann, Proceedings of the 1977 International Symposium on Lepton and Photon Interactions at High Energies, Hamburg, ed. F. Gutbrod (DESY, 1977), p. 811.
27. A.J. Buras, E.G. Floratos, D.A. Ross and C.T. Sachrajda, Nucl. Phys. 131, 308 (1977).
28. E.G. Floratos, D.A. Ross and C.T. Sachrajda, Nucl. Phys. B129, 66 (1977). There are some minor errors in these calculations which do not seem to affect the qualitative phenomenological conclusions. See W.A. Bardeen, A.J. Buras, D. Duke, and T. Muta, FNAL preprint 78/42 THY (1978); also E.G. Floratos, D.A. Ross and C.T. Sachrajda, private communication.
29. O. Nachtmann, Nucl. Phys. B63, 237 (1973) and Nucl. Phys. B78, 455 (1974), S. Wandzura, Nucl. Phys. B122, 412 (1977).
30. To be really sure of this, we need the largest feasible lever arm in Q^2. A good way to realize this is with high energy e-p colliding rings, see for example "CHEEP - an e-p facility in the SPS", CERN Yellow Report 78-02, edited by J. Ellis, B.H. Wiik and K. Hübner (1978).
31. The possibility that high twist operators might give phenomenologically significant scaling violations was discussed in particular by I.A. Schmidt and R. Blankenbecler, Phys. Rev. D16,

1318 (1977).
32. See Georgi and Politzer, ref. 16 and A. De Rújula, H. Georgi and H.D. Politzer, Ann. Phys. 103, 315 (1977); R. Barbieri, J. Ellis, M.K. Gaillard and G.G. Ross, Nucl. Phys. B117, 50 (1977).
33. See D. Bailin and A. Love, Nucl. Phys. B75, 159 (1974); M. Glück and E. Reya, Phys. Rev. D16, 3242 (1977). Abelian vector gluon theories give the same non-singlet anomalous dimensions as QCD in order g^2. Therefore the Table and Figure 7 should best be regarded as evidence for the vector nature of the gluons. The main evidence that the correct theory is QCD rather than an (abelian or non-abelian) vector gluon theory with a non-zero ultra-violet fixed point coupling is the logarithmic Q^2 dependence of the moments discussed earlier.
34. See for example D.H. Perkins, Proceedings of the 16th International Conference on High Energy Physics, Chicago-Batavia 1972 (NAL, Batavia, 1972) p. 189. The fraction is Q^2 dependent: for a more sophisticated evaluation see H.D. Politzer, Nucl. Phys. B122, 237 (1977).
35. H.L. Anderson, H.S. Matis and L.C. Myrianthopoulos, Phys. Rev. Lett. 40, 1061 (1978).
36. The only cloud on the deep inelastic horizon is the apparent discrepancy between QCD calculations (see ref. 32) and measurements of $R=\sigma_L/\sigma_T$ in electroproduction - see L.N. Hand, ref. 24. We hope that this disagreement arises from the systematic problems in making the measurements of R, but we should avoid dogmatism.
37. See for example J. Frenkel, R. Meuldermans, I. Mohammed and J.C. Taylor, Nucl. Phys. B121, 58 (1977); and Section 5 of Marciano and Pagels, ref. 1.
38. T.A. DeGrand, Y.J. Ng and S.-H.H. Tye, Phys. Rev. D16, 3251 (1977).
39. K. Koller and T.F. Walsh, Phys. Letters 72B, 227 (1977), erratum (to be published) and DESY preprint DESY 78/16 (1978); M. Krammer and H. Krasemann, Phys. Lett. 73B, 58 (1978); S.J. Brodsky, D.G. Coyne, T.A. DeGrand and R.R. Horgan, Phys. Lett. 73B, 203 (1978); H. Fritzsch and K.-H. Streng, Phys. Lett. 74B, 90 (1978).
40. A. De Rújula, J. Ellis, E.G. Floratos and M.K. Gaillard, CERN preprint TH 2455 (1978).
41. While foreshadowed in the first two papers of ref. 11, the present surge of interest in this approach in QCD stems from H.D. Politzer, Phys. Lett. 70B, 430 (1977).
42. I.G. Halliday, Nucl. Phys. B103, 343 (1976); H.D. Politzer, Nucl. Phys. B129, 301 (1977); and C.T. Sachrajda, Phys. Lett. 73B, 185 (1978) made some analyses of this process in perturbation theory. Some of their results were anticipated phenomenologically by J.B. Kogut, Phys. Lett. 65B, 377 (1976); I. Hinchcliffe and C.H. Llewellyn Smith, Phys. Lett. 66B, 281 (1977). The most complete analysis is that due to Dokshitzer, D'yakonov and Troyan, ref. 10.
43. An early phenomenological discussion using this philosophy was E.G. Floratos, Nuovo Cimento 43A, 241 (1978). K.H. Craig and

C.H. Llewellyn Smith, Phys. Lett. 72B, 349 (1978) initiate a perturbative justification of the QCD calculation of large p_T jets in deep inelastic leptoproduction. Other phenomenological references are H. Georgi and H.D. Politzer, Phys. Rev. Lett. 40, 4 (1978), G. Altarelli and G. Martinelli, Rome University preprint "Transverse Momentum of Jets in Electroproduction from Quantum Chromodynamics" (1978).

44. C.L. Basham, L.S. Brown, S.D. Ellis and S.T. Love, Washington University preprint RLO-1388-746 (1977).
45. T. Kinoshita, J. Math. Phys. (N.Y.) 3, 650 (1962); T.D. Lee and M. Nauenberg, Phys. Rev. 133, B1549 (1964).
46. The correct specification of the infrared cutoff requires more care than that taken here. Consult ref. 45 and Sterman and Weinberg, ref. 9, for more details.
47. See Sterman and Weinberg, ref. 9.
48. G. Sterman, Stony Brook preprints ITP-SB-77-69, 72 (1977).
49. The basic decay modes of charmonium states are discussed in ref. 3. The observability of 3-jet final states was first discussed in ref. 38: see also references 39 and 40. More consideration should be given to the infrared singularities associated with the initial bound state before these results can be regarded as "rigorous".
50. H. Georgi and M. Machacek, Phys. Rev. Lett. 39, 1237 (1977); E. Farhi, Phys. Rev. Lett. 39, 1587 (1977).
51. Once multi-jet events are observed, one would like to study 3-jet Dalitz plots and so on (see G. Parisi, Phys. Lett. 74B, (1978)): the only problem is how to pick such events out experimentally. For a systematic analysis, see ref. 40.
52. For the moment, this and subsequent factorization statements should be taken as applying in a leading logarithmic approximation.
53. See also Dokshitzer, D'yakonov and Troyan (ref. 10) who discuss two final state hadrons.
54. There will be contributions to $\langle p_T^2 \rangle$ arising from the primordial k_T of the colliding constituents, as well as from QCD perturbative effects. Note that in QCD perturbation theory the p_T of the lepton pair is not necessarily the sum of the k_T of the colliding constituents. See E.L. Berger, Argonne preprint ANL-HEP-PR 78/12 (1978) for a recent phenomenological review.
55. H. Georgi, Harvard University preprint HUTP-77/A090 (1977) makes this warning very strongly. It will be important to do a complete phenomenological analysis. The leading logarithms in $g+q \to \ell^+\ell^-+q$ actually contribute to the $q+q \to \ell^+\ell^-$ subprocess: see Sachrajda, ref. 42.
56. C.T. Sachrajda, CERN preprint TH 2459 (1978); W. Furmanski, private communication and Krakow University preprint to appear. For a related discussion within the CIM framework, see W.E. Caswell, R.R. Horgan and S.J. Brodsky, SLAC preprint PUB-2106 (1978).
57. D. Amati, R. Petronzio and G. Veneziano, CERN preprint TH 2470 (1978) have an elegant demonstration of factorization at the one-loop level, and related arguments for both leading and non-leading

logarithms is being prepared by R.K. Ellis, H. Georgi, M. Machacek, H.D. Politzer, G.G. Ross, private communication.

58. K.M. Bitar and S.-J. Chang, Phys. Rev. D17, 486 (1978) point out that one can formulate tunnelling directly for Minkowski field theory.

59. G. 't Hooft, Phys. Rev. D14, 3432 (1976). The Pauli-Villars regularization scheme is used when evaluating the coefficients in equation (26) (see also references 13 and 14). The parameters Λ and m_i are those defined perturbatively in ref. 16: asymptotically $m_i \sim \bar{m}_i \ (\ln Q^2)^{\frac{-12}{33-2N_f}}$.

60. L.S. Brown, R. Carlitz, D. Creamer and C. Lee, Phys. Lett. 70B, 180 and Washington University Preprint RLO-1388-735 (1977).